Check for updates

Ontogenetic δ^{15}N Trends and Multidecadal Variability in Shells of the Bivalve Mollusk, *Arctica islandica*

Bernd R. Schöne* and Qian Huang*

Institute of Geosciences, University of Mainz, Mainz, Germany

Bulk stable nitrogen isotope values of the carbonate-bound organic matrix in bivalve shells (δ^{15}N$_{CBOM}$) are increasingly used to assess past food web dynamics, track anthropogenic nitrogen pollution and reconstruct hydrographic changes. However, it remains unresolved if the δ^{15}N$_{CBOM}$ values are also affected by directed ontogenetic trends which can bias ecological and environmental interpretations. This very aspect is tested here with modern and fossil specimens of the long-lived ocean quahog, *Arctica islandica*, collected from different sites and water depths in the NE Atlantic Ocean. As demonstrated, δ^{15}N$_{CBOM}$ values from the long chronologies show a general decrease through lifetime by −0.006‰ per year. The most likely reason for the observed δ^{15}N$_{CBOM}$ decline is a change in the type of proteins synthesized at different stages of life, i.e., a gradual shift from proteins rich in strongly fractionating, trophic amino acids during youth toward proteins rich in source amino acids during adulthood. Aside from this ontogenetic trend, distinct seasonal to multidecadal δ^{15}N$_{CBOM}$ variations (ca. 50 to 60 years; up to 2.90‰) were identified. Presumably, the latter were governed by fluctuations in nutrient supply mediated by the Atlantic Multidecadal Variation (AMV) and Atlantic Meridional Overturning Circulation (AMOC) combined with changes in nitrate utilization by photoautotrophs and associated Rayleigh fractionation processes. Findings underline the outstanding potential of bivalve shells in studies of trophic ecology, oceanography and pollution, but also highlight the need for compound-specific isotope analyses.

Keywords: nitrogen isotopes, sclerochronology, particulate organic matter, ontogeny, physiology, periostracum, shell-bound proteins, multidecadal climate variability

INTRODUCTION

The stable nitrogen isotope composition of organic materials serves as a powerful tool in trophic ecology, hydrography and pollution studies (e.g., Fry, 1988; Hobson and Welch, 1992; Ohkouchi et al., 2015; Doherty et al., 2021). For example, as the bulk δ^{15}N value of tissues increases from prey to predator (Miyake and Wada, 1967; DeNiro and Epstein, 1981), on average, by 3.4‰ (Minagawa and Wada, 1984), the trophic position of consumers can be determined, and thus the food web structure and food chain length, provided that the nitrogen isotope baseline (=δ^{15}N value of the primary producers) is known (Fry, 1988; Thompson et al., 1995; Post, 2002; Perkins et al., 2014). Tissue δ^{15}N data can also help to unravel trophic interactions within food webs (Ishikawa, 2018)

and to compute the proportion of different food items in the diet of a consumer, specifically when used in conjunction with other isotope systems (Phillips and Koch, 2002; O'Donnell et al., 2003). Furthermore, tissues register nitrogen isotope changes of total dissolved nitrogen in the water (TDN; δ^{15}N$_{TDN}$) which enables reconstructions of biogeochemical cycles, water mass sources and anthropogenic nitrogen pollution etc. (e.g., Altabet et al., 1995; Voss et al., 2005; Ellis, 2012; Geeraert et al., 2020). With suitable δ^{15}N archives it becomes possible to place all such ecological and environmental changes into precise temporal context, determine the pristine state of ecosystems prior to human perturbations and quantify the anthropogenic impact on ecosystems (e.g., Sherwood et al., 2011; Lueders-Dumont et al., 2018; Wang et al., 2018; Duprey et al., 2020), and test respective ecological models (Duce et al., 2008; Serna et al., 2010).

According to recent sclerochronological studies, shells of bivalve mollusks serve as suitable δ^{15}N archives, because they provide high-resolution (annually and seasonally), temporally well-constrained records of past ecological and environmental changes (Gillikin et al., 2017; Whitney et al., 2019; Das et al., 2021). Both bulk δ^{15}N values of the periostracum (δ^{15}N$_P$) and the carbonate-bound organic matrix of their shells (δ^{15}N$_{CBOM}$) typically correlate strongly with δ^{15}N values of contemporaneous soft tissues (LeBlanc, 1989; O'Donnell et al., 2003; Carmichael et al., 2008; Delong and Thorp, 2009; Watanabe et al., 2009; Kovacs et al., 2010; Versteegh et al., 2011; Graniero et al., 2016, 2021; Darrow et al., 2017), specifically the adductor muscles (Gillikin et al., 2017), and thus also with the diet of the bivalves (δ^{15}N$_{Diet}$) (O'Donnell et al., 2003; Carmichael et al., 2004; Graniero et al., 2021). However, it still remains untested if ontogenetic δ^{15}N trends exist that are linked to changes of the physiology of the bivalve. Such trends could superimpose environmental and ecological signals and bias interpretations. The reason for this assumption is that the protein-amino acid composition of the shell organic matrix varies through lifetime (Goodfriend and Weidman, 2001). Since the different amino acids exhibit vastly different nitrogen isotope fractionation patterns (McClelland and Montoya, 2002; Chikaraishi et al., 2007), a compositional change would inevitably be associated with a shift in bulk δ^{15}N values of shell organics and periostracum.

Here, the hypothesis is tested that bulk δ^{15}N$_{CBOM}$ chronologies of the long-lived bivalve mollusk, *Arctica islandica*, from the Northeast Atlantic are affected by ontogenetic trends. This species can attain a lifespan of several decades to hundreds of years (Thompson et al., 1980; Schöne et al., 2005a; Wanamaker et al., 2008; Butler et al., 2013). Since ecological and ontogenetic shifts can eliminate or reinforce each other, specimens were used that lived during different time intervals in different habitats. Possible reasons for seasonal to multidecadal δ^{15}N$_{CBOM}$ variations are discussed. The δ^{15}N values of shell organics were also compared to such of periostracum. Results of this study can help to improve bivalve shell δ^{15}N-based ecological and environmental reconstructions. Findings highlight the need for compound-specific isotope analysis of shell organic matrices which so far has only rarely been explored (Ellis, 2012; Misarti et al., 2017).

MATERIALS AND METHODS
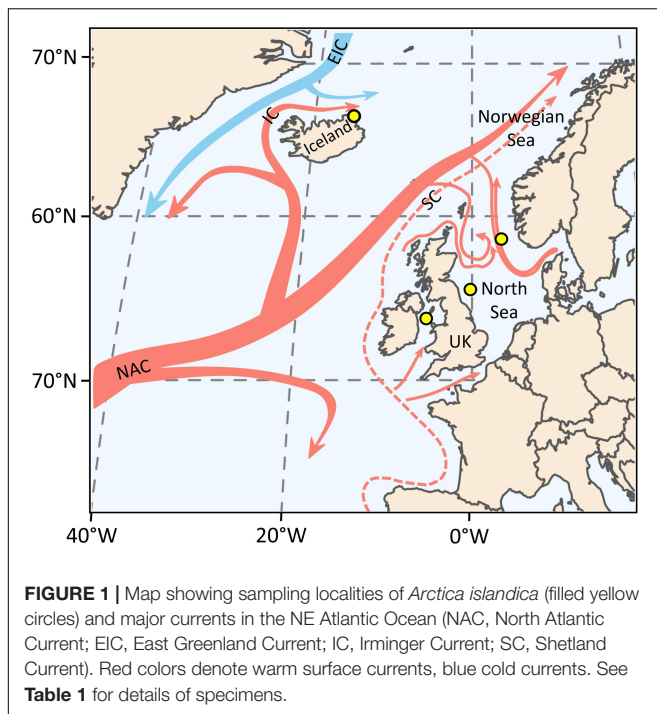
Sample Material

For the current study, shells of four specimens of *Arctica islandica* from different localities and water depths in the North Atlantic Ocean were selected (**Figure 1** and **Table 1**). Two specimens were collected alive from surface waters, one from NE Iceland (þistilfjörður, þórshöfn) and one from the Irish Sea (**Figure 1** and **Table 1**) in August 2012 and July 1868, respectively. The modern specimen (ICE12-05-12 A-L) was eviscerated immediately after collection and both valves then stored in a dry and dark environment. The historical ocean quahog (M071868-A1L) belongs to the Karl August Moebius collection that is curated by the Zoological Museum of the University of Kiel. Details on the exact sample locality, water depth and treatment after collection are not available, but the valves were stored in dry condition when obtained from the museum collection in 2004. In the historical shell, large portions of the periostracum were missing and flaked off from the shell. In addition, single valves of two radiocarbon dated subfossil specimens came from the Fladen Ground (Late Holocene, specimen WH241-604-BoxL-D11R) and the East Farn Deeps (Early Holocene, specimen WH241-677-BoxB-D1R), North Sea (**Figure 1** and **Table 1**). These specimens were collected by bottom trawling from 113 and 79 m water depth, respectively, during cruise no. 20020219 with the R/V "Walther Herwig III" in summer 2002. Uncalibrated radiocarbon ages (Libby years) were 2,840 ± 40 year BP (ontogenetic years 5–9 in specimen WH241-604-BoxL-D11R) and 8,770 ± 50 years BP (years 7–9 of WH241-677-BoxB-D1R). Calibrated ^{14}C ages (cal yr BCE, 2σ) were calculated with CALIB 8.2 ([1]; last access: 28 June 2021; **Table 1**) using the calibration set marine20.14c (Heaton et al., 2020) and ΔR values of −140 ± 35 and −146 ± 68 year, respectively.

Sampling

Prior to sampling, one valve of each specimen was gently rinsed with de-ionized water and allowed to air-dry. No oxidative reagents were used to clean the shells prior to shell powder acquisition. As outlined by Gillikin et al. (2017), in contrast to other, porous bioceramics, bivalve shells are very dense and thus do not require oxidative cleaning. In addition, oxidative agents can potentially alter the isotope composition of shells (Schöne et al., 2017; own unpublished data). Likewise, no acids were used to remove adhering calcium carbonate crystals from periostracum, because this treatment modifies the δ^{15}N values as well (Schlacher and Connolly, 2014; own unpublished data). Data presented here thus represent the δ^{15}N values of both the intercrystalline and intracrystalline organic matrix of the shells.

For reliable identification of shell growth patterns and temporal contextualization of the samples, valves were mounted to Perspex cubes with a fast-curing plastic welder (WIKO Multi Power 03) and surfaces along the axis of maximum growth from the hinge to the ventral margin coated with a ca. 8 mm wide thin layer of high-viscosity WIKO metal epoxy resin 05. Along that axis, the valves were cut with a low-speed precision saw (Buehler

[1]http://calib.org/calib/

FIGURE 1 | Map showing sampling localities of *Arctica islandica* (filled yellow circles) and major currents in the NE Atlantic Ocean (NAC, North Atlantic Current; EIC, East Greenland Current; IC, Irminger Current; SC, Shetland Current). Red colors denote warm surface currents, blue cold currents. See **Table 1** for details of specimens.

Isomet 1000) equipped with a 400 μm thick diamond-coated saw blade (Buehler IsoMet Blade 15LC) at 225 rpm. Cross-sectioned halves were ground on glass plates with SiC suspensions (F800, F1200) and then polished with 1 μm Al_2O_3 powder on a Buehler Microfloc cloth.

Annual shell growth increments and lines guided the acquisition of periostracum and shell powder samples and ensured that isotope data of these samples could be placed in precise temporal context. Schöne (2013) reviewed that growth line formation in *A. islandica* starts ca. 4 weeks after the seasonal temperature maximum and takes ca. 2 months. During this time period, biomineralization rate is extremely slow and may occasionally come to a complete halt (Jones, 1980; Schöne et al., 2005a). Thereafter, growth resumes at slow rate until food availability increases (Thompson et al., 1980;

Schöne et al., 2005a). In surface waters, the main growing season of *A. islandica* covers the time interval from ca. mid-November to mid-September of the following calendar year, while in deeper waters, the main growing season is typically lagged by several months, because the seasonal temperature maximum occurs later than in surface waters (Schöne et al., 2005a,b). The "annual" growth increments of specimens from different water depths thus cover different parts of the year (Schöne et al., 2005a,b).

Sampling was completed with a Rexim Minimo low-speed milling system (ca. 600 rpm) which was firmly attached to a binocular microscope (64 and 160 × magnification). For micromilling, various different drill bits were used: (i) a diamond-coated cylindrical drill bit (1 mm diameter; Gebr. Brasseler GmbH & Co., KG #835 104 010), (ii) a diamond-coated inverted cone (3 mm diameter; 814 104 030) and (iii) a conical SiC drill bit (300 μm at tip; H52 104 003). Periostracum was micromilled from individual "annual" increments in shell portions located posteriorly and anteriorly from the metal epoxy band. In slow-growing shell portions, each periostracum sample represented an average of up to 3 years, in one case 4 years (**Supplementary Material 1**). Furthermore, shell powder samples were taken from the inner portion of the outer shell layer (iOSL). For that purpose, the metal epoxy, periostracum and the outer portion of the outer shell layer (oOSL) were physically removed from one half of each valve. Then, powder samples were micromilled in cross-section, guided by internal growth patterns, to obtain "annual" averages. In fast-growing shell portions near the umbo, samples were obtained by surface micromilling (approx. 1 to 2 cm broad swaths). To assess the seasonal δ^{15}N variance, subannual samples were obtained in some fast-growing shell portions. In slow growing shell portions near the ventral margin of the oldest-grown subfossil specimen, each shell powder sample contained up to 6 years (**Supplementary Material 1**).

It should be pointed out that this kind of shell powder sampling was extremely time-consuming (i.e., 30 to 60 min per sample), because micromilling had to be extremely precise to minimize unwanted time-averaging and proceed very gently to avoid too much frictional heat. Depending on column size (large-volume or small-volume method, see further below) approx. 5.0 to 16.7 mg or 2.4 to 4.0 mg of shell powder were required

TABLE 1 | Overview of samples of *Arctica islandica* used in the present study.

Specimen ID	Locality, Lat/lon	Water depth (m)	Date of collection	^{14}C sample from ontogenetic years	Uncalibrated ^{14}C age (yr BP), [ΔR (year)]	2σ calibrated ^{14}C age (cal yr BCE) range (median)
ICE12-05-12 A-L	NE Iceland, 66°09′58.92″N, 015°22′58.92″W	9	20 Aug. 2012			
M071868-A1L	Irish Sea	30–50?	July 1868			
WH241-604-BoxL-D11R	Fladen Ground, 58°43.68′N, 002°39.35′E	113	24 June 2002	5 to 9	2,840 ± 40 (−140 ± 35)	797–428 (637)
WH241-677-BoxB-D1R	East Farn Deeps, 55°23.91′N, 000°01.84′W	79	6 Aug. 2002	7 to 9	8,770 ± 50 (−146 ± 68)	7,706–7,213 (7,471)

A, D, L, and R in suffix of specimen IDs denote collected alive or dead, left and right valve, respectively.
Subfossil specimens were provided by Ingrid Kröncke (Senckenberg, Wilhelmshaven, Germany), the historical shell by Wolfgang Dreyer (formerly Zoological Museum Kiel, Germany), and the modern specimen by Soraya Marali and Hilmar Holland (formerly Univ. of Mainz).

per analysis (total number of shell powder analyses = 249). To measure the periostracum samples (N = 47), 82 to 1,733 μg and 45 to 280 μg were processed per analysis (total number of periostracum analyses = 83), depending on EA method (see below). The total number of samples equaled 201. Of such, 41 were measured in triplicate and 49 in duplicate (**Table 2** and **Supplementary Materials 1, 2**).

Nitrogen Stable Isotope Measurements

Powdered samples were weighted into tin capsules and measured on a Thermo Scientific MAT 253 continuous-flow isotope ratio mass spectrometer coupled to an elemental analyzer (Thermo Scientific Flash EA 2000) equipped with a Costech zero blank autosampler at the Institute of Geosciences, University of Mainz, Germany. Samples were combusted in the EA at a temperature of 1,020°C (reduction column temperature: 650°C). 85 analyses of samples were completed with the standard column (large-volume method, hereafter referred to as Lvol-EA), the remaining 247 analyses of samples with a small-volume setup (Svol-EA; column outer diameter: 10.5 tapered to 6 mm, column inner diameter: 7.2 tapered to 1.8 mm, #IVA4680090001 distributed by IVA Analysentechnik GmbH & Co., KG), similar to the nano-EA setup described in Polissar et al. (2009). The Svol-EA method required approx. three times less sample material than the Lvol-EA method [shell powder of iOSL of *A. islandica*: 9.6 ± 3.8 mg (N = 56) vs. 3.8 ± 0.3 mg (N = 193) (average ± 1σ); periostracum: 473 ± 330 (N = 29) vs. 133 ± 79 μg (N = 54)] to attain signal intensities (amplitude m/z 28) of approx. 305 mV (shell powder) and up to 1,155 mV (periostracum); note, even small amounts of adhering shell powder resulted in lower signal heights, because CaCO$_3$ is much heavier than periostracum (for data summary see **Supplementary Materials 1, 2**). The analyses of the international standard, USGS43 demonstrate that measurements provided by the Svol-EA method are accurate. The significant reduction of sample material using the Svol-EA method improves the temporal resolution by reducing the time-averaging of each sample, which is highly beneficial for the analysis of nitrogen isotope chronologies derived from bivalve shells.

Raw isotope data were corrected using a two-point correction method with L-glutamic acid reference standards, USGS40 (δ^{15}N: −4.52‰) and USGS41 (δ^{15}N: +47.57‰) or USGS41a (δ^{15}N: +47.55‰), with m/z 28 signal intensities in the range of the analytes, and reported in per mil versus air. Four calibration batches containing triplicates of USGS40 and USGS41 (or 41a) were equally distributed across each analytical session: one calibration batch at the beginning and end, respectively, and two additional batches after each 21 to 24 samples. Quality control was accomplished with blindly measured USGS43 (Indian Human Hair; δ^{15}N: +8.44‰) that were measured— typically in triplicate—along with the samples (N = 31; accuracy = 0.08 ± 0.11‰, precision = 0.09 ± 0.02‰).

As previously noted by Gillikin et al. (2017), the analytical error of the reference materials increases with decreasing signal intensity, and this relationship can provide information on the potential analytical error of the samples. For that purpose, the 1σ precision errors of the means of the reference material triplicates (35 triplicates of USGS40, 17 of USGS41, 18 of USGS41a, and 10 of USGS23) were plotted against the average mass 28 signal intensities of the respective triplicates and the data fitted with a power function (R = 0.56; p < 0.001) (Equation 1):

$$EPE = 6.7295 \cdot ampl28^{-0.699}. \qquad (1)$$

With this non-linear equation, the estimated precision error (*EPE*) of a sample can be approximated from its signal intensity on mass 28 (*ampl28* in mV). On average, the analytical precision (1σ) was better than 0.20 and 0.13‰ for shell powders and better than 0.11 and 0.05‰ for periostracum using the Lvol and Svol-EA methods, respectively. The precision errors ranged between 0.06 and 0.37‰ for shell powder, and between 0.03 and 0.26‰ for periostracum. In cases where an average value was computed from multiple measurements of the same sample, the variance of the aliquots needs to be taken into consideration, i.e., the respective error needs to be propagated. Actually, 41 samples were run in triplicate, 49 in duplicate and the remaining 111 only once (note, all Lvol-EA samples belong to the latter group). On average, the mean of the triplicates came with a 1σ precision error of 0.22‰ partly reflecting sample inhomogeneities. To provide a conservative error estimate, the estimated precision errors of all samples that were measured less than thrice were propagated with this average 1σ precision error (0.22‰) resulting

TABLE 2 | Overview of numbers of stable nitrogen isotope samples and measurements completed in the four *Arctica islandica* specimens.

Specimen ID, locality	Measurements (N = 332)					Samples (N = 201)				
	CBOM: 249		Periostracum: 83			Triplicates: 41		Duplicates: 49	Single: 111	
	LVol: 56	SVol: 193	LVol:29	SVol:54		CBOM	P	CBOM	CBOM	P
ICE12-05-12 A-L,NE Iceland	33		29						33	29
M071868-A1L,Irish Sea	19			54			18		19	
WH241-604-BoxL-D11R,Fladen Ground	4	89				17		19	4	
WH241-677-BoxB-D1R,East Farn Deeps		104				6		30	26	
	↓	↓	↓	↓		↓	↓	↓	↓	↓
Σ LVol measurements	56		29		→ 85 Σ	23	18	49	82	29
Σ SVol measurements		193		54	→ 247					

CBOM, shell carbonate-bound organic matrix; P, periostracum; Σ, sum; LVol, SVol, Large, small-volume EA-method.

in an average propagated uncertainty of 0.26‰ (for details see **Supplementary Material 2**).

Nitrogen concentrations (**Supplementary Material 2**) were computed based on various weights of L-glutamic acid (9.52 wt%). Accordingly, shell powders contained, on average, 761 ± 305 ppm by weight (or μg/g; = 0.076 wt%) nitrogen (range: 305 to 1,846 ppm by weight = 0.031 to 0.185 wt%), whereas periostracum contained, on average, 8.79 ± 3.32 wt% N (range: 2.74 to 15.63 wt%).

Statistical Analysis

The potential trend in δ^{15}N$_{CBOM}$ and δ^{15}N$_P$ time-series was examined and quantified by linear regression with Pearson's correlation coefficient and associated *p*-value (df = n −2). To examine the differences between δ^{15}N$_{CBOM}$ and δ^{15}N$_P$, a two-way Analysis of Variance (ANOVA) was conducted with two factors considered: (1) Tissues—carbonate and periostracum; (2) Shells—from NE Iceland and the Irish Sea, followed by pairwise comparisons. The assumption of normality and homogeneity of variances were diagnosed with Kolmogorov-Smirnov tests and Levene's tests, respectively. Analyses were conducted using packages stats (R Core Team, 2021) and car (Fox and Weisberg, 2019) in the R software version 3.6.3 (R Core Team, 2021). Spectral analysis (Fourier transformation, Lomb periodogram) was conducted to quantify the periodic oscillations in the time-series of the two long δ^{15}N$_{CBOM}$ series of shells from the Fladen Ground and the E Farn Deeps. The same analysis was performed with Atlantic Multidecadal Variation (AMV) index.

RESULTS

The modern bivalve from NE Iceland (ICE12-05-12 A-L) and the historical specimen from the Irish Sea (M071868-A1L) attained a lifespan of merely 33 years, whereas the two subfossil *A. islandica* specimens lived for 92 (Fladen Ground, WH241-604-BoxL-D11R) and 162 years (E Farn Deeps, WH241-677-BoxB-D1R) based on annual increment counts (**Figure 2** and **Table 3**). δ^{15}N$_{CBOM}$ chronologies of the shells from NE Iceland, the Fladen Ground and the E Farn Deeps showed a general and statistically significant decrease through ontogeny which were estimated with linear regression models (**Table 3**). The specimens from the Fladen Ground and the E Farn Deeps shared a common weak trend (−0.006‰ year^{-1}), while the decreasing trend occurred more than ninefold stronger in the NE Icelandic shell (−0.057‰ year^{-1}). A weak decline in δ^{15}N$_{CBOM}$ was also observed in the shell from the Irish Sea (−0.008‰ year^{-1}), yet the trend is not statistically significant (**Table 3**).

The two long chronologies showed markedly larger inter-annual variance during early ontogeny than later during life and seemed to exhibit an initial δ^{15}N$_{CBOM}$ increase by up to approx. 1.41‰ (+0.071 and +0.064‰ year^{-1}, respectively) until the age of 20 or so, followed by a gradual decline (**Figures 2C,D**). It should be noted that the increase in δ^{15}N$_{CBOM}$ which is coincidental with early ontogeny of *A. islandica* also fits into the multidecadal cycle throughout both records (See further). In the two shorter-lived specimens, such inflection points were

not evident or superimposed by low-frequency components (see below) (**Figures 2A,B**).

Besides these potential ontogenetic trends, the two longer time-series also showed distinct multidecadal oscillations with a period length approx. 50 to 60 years and quasi-decadal variability at ca. 12–16 years as well as amplitudes ranging between 1.80 and 2.90‰ (**Figures 2**, **3** and **Supplementary Material 1**). A statistically sound spectral analysis of this low-frequency variability, however, would require longer time-series (95% confidence levels were barely reached, **Figure 3**). Furthermore, high-resolution sampling in a few annual increments of specimens from Iceland and the E Farn Deeps offered an insight into the seasonal variability. As demonstrated by **Figures 2A,D**, on seasonal time-scales, the δ^{15}N$_{CBOM}$ data fluctuated almost an order of magnitude stronger (more than 2.50‰) than from year to year (0.35‰).
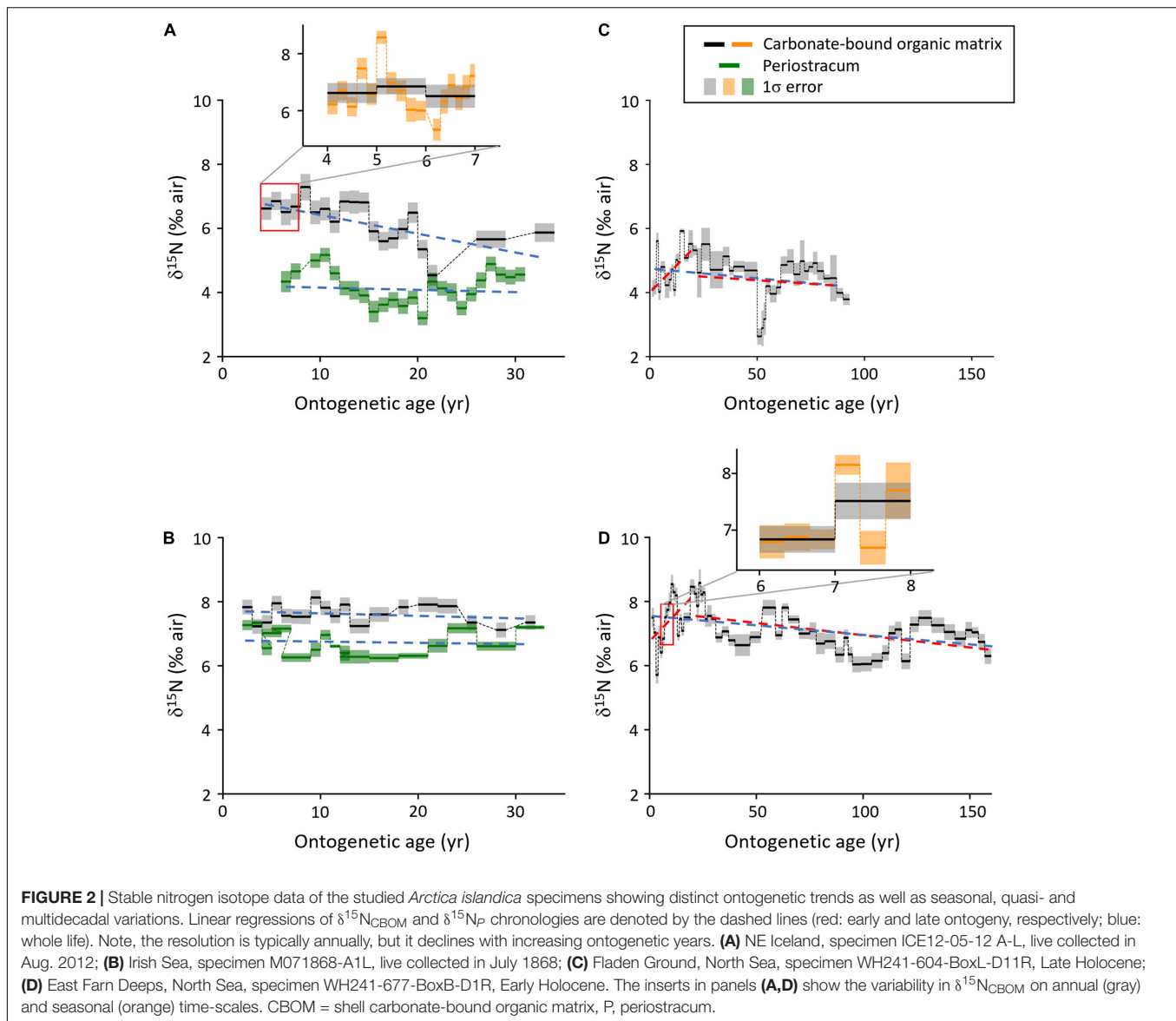
The largest δ^{15}N$_{CBOM}$ difference (annual averages) through lifetime was observed in the specimen from the Fladen Ground (+2.63‰ to +5.92‰ = 3.29‰), followed by shells from NE Iceland (+4.54‰ to +7.29‰) and the E Farn Deeps (+5.71‰ to +8.58‰), both with an average range of approx. 2.90‰. A significantly lower spread of only 1.01‰ was found in the specimen from the Irish Sea (+7.12 and +8.13‰) (**Figure 2** and **Table 3**).

Periostracum was only preserved in the two live-collected shells from NE Iceland and the Irish Sea. Ontogenetic δ^{15}N trends in periostracum were statistically insignificant yet somewhat showing a weak declining tendency, i.e., −0.007 and −0.006‰ year^{-1}, respectively (**Table 3**). As in shell organics, the δ^{15}N$_P$ range was larger in the NE Icelandic specimen (1.97‰, +3.20 to +5.17‰) than in the shell from the Irish Sea (1.10, +6.24, and 7.34‰). In both specimens, the periostracum was depleted in ^{15}N relative to shell organics (NE Iceland: −2.07‰, Irish Sea: −0.86‰) (**Figure 4** and **Table 3**). Low-frequency changes of the δ^{15}N$_P$ and shell δ^{15}N$_{CBOM}$ chronologies showed some visual agreement, but the correlation was neither strong nor significant (**Figure 2**).

DISCUSSION

The ontogenetic δ^{15}N$_{CBOM}$ decline was most clearly developed in the two old-grown specimens (92 and 162 years-old) (**Figure 2**), and the slopes of their regression lines were similar (approx. −0.60‰ per century; **Table 3**). Irrespective of locality, water depth and time of growth, shell δ^{15}N$_{CBOM}$ values of these two long records declined through lifetime, suggesting a physiological cause and precluding low-frequency climate swings. In comparison, the ontogenetic δ^{15}N$_{CBOM}$ trends from the two short-lived modern specimens might be influenced by the decadal fluctuations, anthropogenic and/or other environmental impacts.

In addition, the time-series revealed pronounced seasonal and multidecadal variability. The latter was best observed in the two long chronologies and comprised period lengths of ca. 50 to 60 years with considerable amplitudes of as much as almost 2.90‰ (**Figure 2**). It should be pointed out that

FIGURE 2 | Stable nitrogen isotope data of the studied *Arctica islandica* specimens showing distinct ontogenetic trends as well as seasonal, quasi- and multidecadal variations. Linear regressions of δ^{15}N$_{CBOM}$ and δ^{15}N$_P$ chronologies are denoted by the dashed lines (red: early and late ontogeny, respectively; blue: whole life). Note, the resolution is typically annually, but it declines with increasing ontogenetic years. **(A)** NE Iceland, specimen ICE12-05-12 A-L, live collected in Aug. 2012; **(B)** Irish Sea, specimen M071868-A1L, live collected in July 1868; **(C)** Fladen Ground, North Sea, specimen WH241-604-BoxL-D11R, Late Holocene; **(D)** East Farn Deeps, North Sea, specimen WH241-677-BoxB-D1R, Early Holocene. The inserts in panels **(A,D)** show the variability in δ^{15}N$_{CBOM}$ on annual (gray) and seasonal (orange) time-scales. CBOM = shell carbonate-bound organic matrix, P, periostracum.

the lifespan of these two bivalves covered two and three full cycles of multidecadal oscillations, respectively, suggesting the observed ontogenetic δ^{15}N$_{CBOM}$ trends are unrelated to environmental changes. In short δ^{15}N$_{CBOM}$ chronologies, fractions of such multidecadal oscillations can exaggerate or be misinterpreted as ontogenetic trends. This can explain the nine-fold stronger ontogenetic δ^{15}N$_{CBOM}$ decrease (6.09‰ per century) in the shell from Iceland (**Table 3**). Thus, in order to disentangle multidecadal shell δ^{15}N$_{CBOM}$ fluctuations from directed ontogenetic trends, it is crucial to study shells of sufficiently long-lived specimens.

Possible Causes for the Ontogenetic δ^{15}NC$_{BOM}$ Trends

The most pressing question is what caused the ontogenetic δ^{15}N$_{CBOM}$ decline. The nitrogen isotope composition of calcium

carbonate-bound organics, which mainly consists of proteins (Goulletquer and Wolowicz, 1989), can be influenced by a variety of different environmental and physiological factors including but not limited to the (1) isotope signature of total dissolved nitrogen (δ^{15}N$_{TDN}$), (2) composition of the diet of bivalves, (3) metabolic/turnover rate (4), reproduction, and (5) protein synthesis.

The changes in environmental δ^{15}N$_{TDN}$ and diet composition of bivalves can be subsumed under extrinsic factors. A shift in the isotope composition of total dissolved nitrogen [i.e., the sum of dissolved inorganic N (ammonium, nitrate, nitrite) and dissolved organic N (urea, amino acids etc.)] becomes encoded in photoautotrophs (phytoplankton, benthic algae etc.) and is subsequently imparted to all consumers including bivalves. Thus, the isotopic level of all components of the food web will change proportionately to the shift in δ^{15}N$_{TDN}$ (e.g., Ohkouchi et al., 2015). Possible reasons for δ^{15}N$_{TDN}$ fluctuations include changes

TABLE 3 | Stable nitrogen isotope statistics of studied *Arctica islandica* specimens.

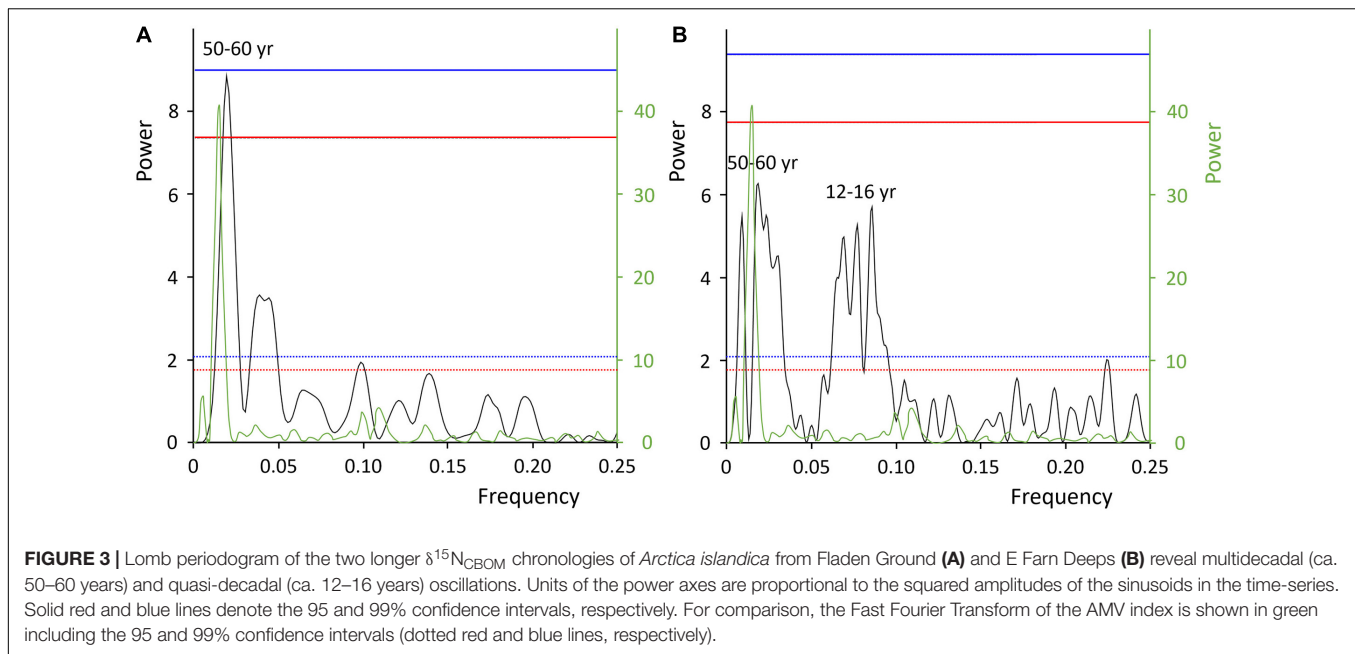| Specimen, locality	Lifespan (year)	δ^{15}N of carbonate-bound organic matrix						δ^{15}N of periostracum						CBOM-P
		Slope (‰/year^{-1})	Shift per century	Variance	Average	r	p	Slope (‰/year^{-1})	Shift per century	Variance	Average	r	p	
ICE12-05-12 A-L, NE Iceland	33	−0.057	−6.09	2.75	6.24	−0.65	0.002	−0.007	−0.52	1.97	4.17	−0.10	0.650	2.07
M071868-A1L, Irish Sea	33	−0.008	−0.75	1.01	7.61	−0.23	0.351	−0.006	−0.62	1.10	6.75	−0.14	0.586	0.86
WH241-604-BoxL-D11R, Fladen Ground	92	−0.006	−0.60	3.29	4.56	−0.26	0.011							
WH241-677-BoxB-D1R, East Farn Deeps	162	−0.006	−0.60	2.87	7.19	−0.44	<0.001							

CBOM, shell carbonate-bound organic matrix; P, periostracum.
If not otherwise indicated, all δ^{15}N values are given in per mil vs air (‰).

in ocean circulation, mixed layer depth, upwelling, pH value, nitrogen cycling processes, influx of freshwater and input of anthropogenic nitrogen by atmospheric deposition or through rivers (e.g., Altabet et al., 1995; Cabana and Rasmussen, 1996; Voss et al., 2005; Sherwood et al., 2011; Ellis, 2012; Wang et al., 2018; Whitney et al., 2019; Duprey et al., 2020; Hopkins et al., 2020; Doherty et al., 2021). In addition, the δ^{15}N value of bivalve soft tissues can also be affected by changes in the dietary composition of the bivalve (e.g., Kang et al., 1999; Tue et al., 2012). As a suspension-feeder, *A. islandica* generally feed on suspended POM (Josefson et al., 1995; Cargnelli et al., 1999), representing a mixture of zooplankton, phytoplankton, bacteria, benthic algae and organic detritus (Simon et al., 2002; Verdugo et al., 2004). The nitrogen isotope value of POM depends highly on the community structure of the phytoplankton, because each photoautotroph species exhibits distinct nitrogen isotope fractionation patterns and thus comes with distinct δ^{15}N values (Montoya and McCarthy, 1995; Chikaraishi et al., 2009; Ohkouchi et al., 2015).

However, the above listed extrinsic aspects fail to convincingly explain the common ontogenetic δ^{15}N$_{CBOM}$ decrease in the studied *A. islandica* specimens, simply because it would require that δ^{15}N changes in TDN or diet had occurred at the same rate, magnitude and direction in geographically distant settings and during different time intervals of the past. Such coincidence would be highly unlikely. It appears more reasonable that the ontogenetic nitrogen isotope shifts in shells of *A. islandica* were triggered by physiological factors, e.g., changes in dietary preferences or food selection capabilities through lifetime.

Yet, a change in the composition of potential food items is not necessarily mirrored 1:1 in δ^{15}N$_{CBOM}$ values, nor does an unchanged composition of available food items lead to invariant δ^{15}N$_{CBOM}$ values. Actually, most bivalves do not indiscriminately feed on offered organic substances, but can select food items before or after ingestion (e.g., Kiørboe and Møhlenberg, 1981; Shumway et al., 1985). Based on shell ^{14}C/^{12}C data, Erlenkeuser (1976) concluded that ocean quahogs are "real gourmets which feed on the most recent organic matter only." The food selection capability of *A. islandica* has subsequently been experimentally studied under laboratory conditions. For example, according to Shumway et al. (1985), this species conducts a pre-ingestive selection of organic particles with its labial palps. A constraint that should be mentioned, however, is that the labial palps are very short in *A. islandica* and particle selection capabilities thus less effective than in many other species (Kiørboe and Møhlenberg, 1981). No study has yet investigated in detail if food preferences of the ocean quahog change during lifetime. Respective behavioral changes are commonly observed in facultative deposit feeders and relate to the ontogenetic growth of siphons and labial palps. While juveniles predominantly graze on the seabed, adults with larger siphons filter-feed suspended seston (Rossi et al., 2004; Tue et al., 2012). Perhaps, in *A. islandica*, the preference for phytoplankton and/or the capability to select food particles gradually increases during ontogeny as a consequence of larger labial palps and siphons. If that assumption holds true, *A. islandica* may consume an increasingly larger proportion of food items that are depleted

FIGURE 3 | Lomb periodogram of the two longer δ^{15}N$_{CBOM}$ chronologies of *Arctica islandica* from Fladen Ground **(A)** and E Farn Deeps **(B)** reveal multidecadal (ca. 50–60 years) and quasi-decadal (ca. 12–16 years) oscillations. Units of the power axes are proportional to the squared amplitudes of the sinusoids in the time-series. Solid red and blue lines denote the 95 and 99% confidence intervals, respectively. For comparison, the Fast Fourier Transform of the AMV index is shown in green including the 95 and 99% confidence intervals (dotted red and blue lines, respectively).

in ^{15}N, i.e., more fresh phytoplankton and less organic detritus, resulting in gradually lower δ^{15}N$_{CBOM}$ values as it grows older.

While the hypotheses on changing food preferences and particle selection capabilities can explain the declining values, they fail to elucidate the observed increase in δ^{15}N$_{CBOM}$ values of some shells prior to the age of 20 (**Figures 2C,D**). Changes in the allocation of energy to different compartments (somatic growth, reproduction, maintenance etc.) during ontogeny and associated changes in turnover rate offer a more convincing explanation of the observed isotope patterns. Such changes are described by combined Dynamic Energy Budget and Dynamic

FIGURE 4 | Boxplots showing stable nitrogen isotope offset between carbonate-bound organic matrix and periostracum of live-collected *Arctica islandica* specimens from NE Iceland and the Irish Sea.

Isotope Budget models (Emmery et al., 2011). For example, during early youth, most energy is allocated to somatic growth, while energy flows predominantly into the production of eggs and sperms once maturity is reached (see below), provided that enough food is available. If energy supply is limited (= less food available), somatic maintenance is prioritized over body growth and reproduction (Emmery et al., 2011). Energy availability determines the metabolic rate in the respective compartment and affects isotopic fractionation patterns. In small, young individuals, the structural volume of the body is lower and tissue turnover rates are higher than in larger, older specimens resulting in lower bulk δ^{15}N values in tissues. With the increase in body size, the overall turnover rate decreases and—due to stronger isotope fractionation—tissues get gradually enriched in ^{15}N (Emmery et al., 2011). While this model could potentially explain the observed rise of shell δ^{15}N$_{CBOM}$ values until the age of 20, it cannot be completely ruled out that such increasing trend might also be coincidental with the multidecadal δ^{15}N$_{CBOM}$ variations due to extrinsic factors, which also observed in other parts of the record, e.g., 50–92 years in shell from the Fladen Ground (See sections "Seasonal to Multidecadal Variability" and "Variation of δ^{15}N$_{CBOM}$ in Modern Shells" for more details).

Furthermore, the gradual change of the δ^{15}N$_{CBOM}$ slope at around age 20 could be due to a gradual re-routing of energy from somatic growth to reproduction and/or a change in food preferences and particle selection capabilities (see above). Age 20 is nearly in the middle of the range at which *A. islandica* reaches sexual maturity (Thorarinsdóttir and Steingrímsson, 2000) and somatic growth strongly diminishes associated with major metabolic reorganizations (Abele et al., 2008). Since the gametes, especially eggs, mainly consist of proteins (Baptista et al., 2014) and the heavier nitrogen isotope typically becomes enriched in the proteins, the soft tissues and shell organics would become depleted in ^{15}N during gametogenesis. Yet, this
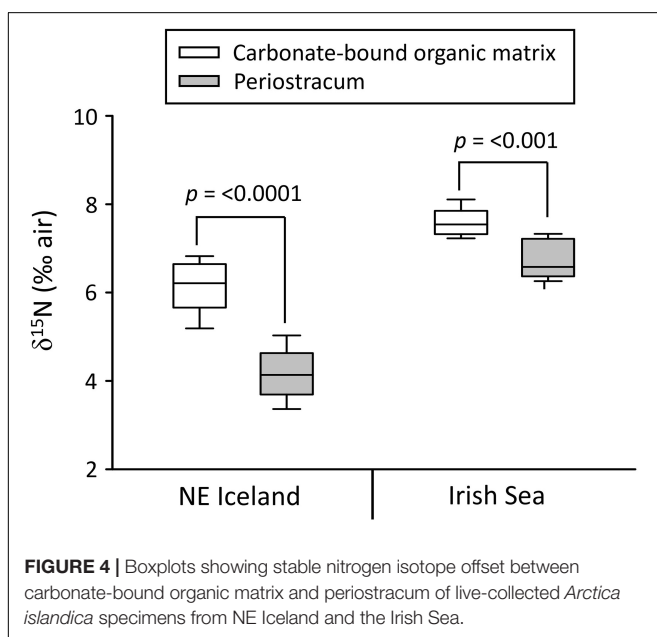
hypothesis still does not fully explain why the $\delta^{15}N_{CBOM}$ values continue to decline thereafter, unless an increasingly larger amount of energy is allocated to reproduction or the capability to select particles becomes increasingly more sophisticated as the bivalve grows older.

A more likely explanation for the general ontogenetic decrease of $\delta^{15}N_{CBOM}$ values after the onset of sexual maturity (or even for the entire chronology if the initial rise in $\delta^{15}N_{CBOM}$ values was an artifact of superimposed multidecadal variability) is that different proteins were synthesized during different stages of life, which aided in the biomineralization process and became included in the shell organics. In fact, the composition of amino acids, the building blocks of proteins, varies over lifetime. In *A. islandica*, glutamic acid (Glu), aspartic acid (Asp) and Alanine (Ala) facilitating crystal growth are favored during fast growth in early ontogeny, whereas the relative proportion of Phenylalanine (Phe), Tyrosine (Tyr) and Lysine (Lys) enhancing shell strength increases in shell organics later during ontogeny (Goodfriend and Weidman, 2001). The different amino acids differ strongly in their $\delta^{15}N$ value, because they undergo specific nitrogen metabolic processes (McClelland and Montoya, 2002; Chikaraishi et al., 2007, 2009). During trophic transfer, the so-called "trophic amino acids" (Popp et al., 2007) (Glu, Asp and Ala) experience strong nitrogen isotopic fractionation (TDF = 8‰ in case of Glu). These amino acids are synthesized *de novo* by consumers and record the isotope signature of the diet. In contrast, the so-called "source amino acids" (Popp et al., 2007) (Phe, Tyr and Lys) can only be fabricated by microorganisms (and plants) and are absorbed by consumers with minimal isotopic fractionation (TDF = 0.4‰ in case of Phe). Their original isotope signature imparted by the primary producers is thus largely preserved at higher trophic positions. In brief, Glu, Asp and Ala are enriched in ^{15}N, whereas Phe, Tyr and Lys are depleted in this isotope. Therefore, the prevalence of trophic amino acids in shell portions laid down during early ontogeny would explain the higher bulk $\delta^{15}N_{CBOM}$ values, whereas the relative increase of weakly fractionating source amino acids later during life resulted in an ontogenetic decrease of bulk $\delta^{15}N_{CBOM}$ values. It would be worth testing this interpretation in future studies through the use of protein amino acid-specific (compound-specific) nitrogen isotope analyses by examining amino acid composition as well as the $\delta^{15}N$ values of each amino acid through the lifetime of the *A. islandica* shells.

Seasonal to Multidecadal Variability

Aside from ontogenetic trends, $\delta^{15}N_{CBOM}$ data varied on seasonal, interannual and multidecadal time-scales (**Figure 2**), which certainly merits further attention in subsequent studies. A detailed analysis of the possible causes for such variations, especially the longer-term variations require a larger number of long $\delta^{15}N_{CBOM}$ chronologies from modern specimens along with high-resolution environmental, ecological and physiological data. Some considerations for the observed $\delta^{15}N_{CBOM}$ patterns are laid out in the following.

It cannot be ruled out that the seasonal to multidecadal $\delta^{15}N_{CBOM}$ variability was linked to physiological changes

discussed earlier, but a response to extrinsic factors, $\delta^{15}N_{Diet}$ and $\delta^{15}N_{TDN}$, appears more reasonable. A likely candidate for the observed seasonal $\delta^{15}N_{CBOM}$ fluctuations includes changes in the isotopic composition of the food of the bivalves, i.e., $\delta^{15}N_{Diet}$. Due to Rayleigh fractionation kinetics during primary production, phytoplankton formed at the beginning of the bloom thus have a lower $\delta^{15}N$ value than such formed near the end of the bloom when the nitrate pool is exhausted, because photoautotrophs preferably assimilate ^{15}N-depleted nitrate (Altabet and Francois, 1994). This isotope range could be reflected in the diet of the bivalves. Additional variability in $\delta^{15}N_{Diet}$ can arise from seasonally varying phytoplankton community structures induced by the physical conditions of seawater, e.g., nutrient levels, light penetration and stratification (Barton et al., 2014). Since the different species are isotopically distinct (Needoba et al., 2003; see also overview in Chikaraishi et al., 2009), a change in phytoplankton species composition throughout the year can cause variations of $\delta^{15}N_{Diet}$, and eventually $\delta^{15}N_{CBOM}$. Furthermore, during different seasons, phytoplankton can assimilate different nitrogen species (Bronk and Glibert, 1993), which can also lead to a considerable variance of the $\delta^{15}N$ baseline.

The most prominent pattern in the isotope chronologies aside from ontogenetic trends was a distinct multidecadal $\delta^{15}N_{CBOM}$ variability. These low-frequency changes could mirror fluctuations of $\delta^{15}N_{TDN}$ values induced by changes in water mass source. For example, a southward shift of the Polar Front would result in a larger proportion of Arctic waters reaching the study site in NE Iceland with the East Greenland Current. In contrast, a northward shift of the Polar Front would increase the influence of Atlantic waters mediated by the Irminger Current (Marali and Schöne, 2015). Arctic waters carry a higher $\delta^{15}N_{TDN}$ signature (Hansen et al., 2012; ca. 6–8‰: Lehmann et al., 2019) than Atlantic waters (4‰, Marconi et al., 2019) and this environmental isotopic baseline shift would be reflected in the entire food web. However, this explanation would not apply to the specimens from the remaining three sites which were only fed by Atlantic waters (**Figure 1**).

More likely, the multidecadal $\delta^{15}N_{CBOM}$ variations reflect shifts in the dietary composition of the bivalves. In fact, changes in phytoplankton species composition are not only known from seasonal, but also interannual and longer time-scales (e.g., Benedetti et al., 2019). However, the underlying controls of long-term changes of the phytoplankton community structure remain less clear. Potential causes include temperature-induced changes in zooplankton assemblages preying on phytoplankton and variations in ocean circulation (Barton et al., 2014), wind-driven changes of the mixed-layer depth affecting the timing of the phytoplankton bloom (Henson et al., 2009) and resource competition dynamics among primary producers (Benedetti et al., 2019). Doherty et al. (2021) recently suggested that fluctuations in nitrate utilization controlled by nitrate supply and changes in large-scale circulation patterns could have caused $\delta^{15}N$ patterns observed in a six-hundred-year coralline red algae record from the Labrador shelf. Following their arguments, a larger proportion of nutrient-poor polar waters delivered by the Labrador current resulted in a complete utilization of nitrate

and δ^{15}N values in algae as high as δ^{15}N of nitrate. In contrast, an increased advective supply of relatively nutrient-rich Atlantic waters caused the opposite. These hydrographic changes were coupled with the Atlantic Multidecadal Variation (AMV) and Atlantic Meridional Overturning Circulation (AMOC): Polar waters dominated during negative AMV phases (corresponding to negative SST anomalies in the northern North Atlantic) and weak AMOC, whereas Atlantic waters prevailed when the AMV was in its positive state and the AMOC strong (note, AMV and AMOC are positively coupled, Zhang et al., 2019). The AMV index describes longer-term variations of sea surface temperature (SST) in the North Atlantic Ocean (Schlesinger and Ramankutty, 1994) that appear to be forced by volcanic activity (Birkel et al., 2016; Mann et al., 2021) and vary within a frequency band corresponding to periods of 50 to 70 years (Schlesinger and Ramankutty, 1994; Delworth and Mann, 2000; Keenlyside et al., 2008; Mann et al., 2021).

Interestingly, the period length of the multidecadal δ^{15}N$_{CBOM}$ cycles of *A. islandica* (**Figure 3**) falls in the same range as that of the AMV (**Figure 5**). A direct comparison with the AMV index, which could shed more light on a potential link between the two records, however, is only meaningful with the NE Iceland δ^{15}N$_{CBOM}$ chronology. The lifespan of all other specimens does not overlap sufficiently long or not at all with the AMV, which is computed from instrumental SST data and thus only covers the time interval since 1856 CE. Although the short NE Iceland δ^{15}N$_{CBOM}$ chronology showed a strong (visual) inverse covariation with the AMV, not just in the low-frequency band (multidecadal component), but also on quasi-decadal time-scales (**Figure 5**). To verify this coupling, longer shell nitrogen isotope time-series of modern *A. islandica* are certainly needed.

In anticipation of a verification of this finding in future studies, some thoughts are provided in the following that could explain an inverse relationship between δ^{15}N$_{CBOM}$ data and the AMV. These ideas were inspired by the works of Edwards et al. (2001); Barton et al. (2003) and Doherty et al. (2021). During negative AMV phases and weak AMOC, lower (ocean and air) temperatures and stronger northerly winds resulted in intensified vertical mixing and delayed water column stratification with negative effects on primary production (Sverdrup, 1953: critical-depth concept). In response to a sluggish meridional circulation, the supply of relatively nutrient-rich Atlantic waters onto the NE Atlantic shelf areas was decreased. Thus, nitrate became depleted and completely utilized by photoautotrophs leading to δ^{15}N$_{Diet}$ and δ^{15}N$_{CBOM}$ values as high as δ^{15}N of nitrate. In contrast, during positive AMV phases and stronger AMOC, warmer water promoted water column stratification and a shallow mixed-layer depth early in the year. The increased AMOC-mediated advection of nutrient-rich Atlantic water caused a surplus of nitrate in surface waters that was only incompletely consumed leading to lower δ^{15}N$_{Diet}$ and δ^{15}N$_{CBOM}$ values. The quasi-decadal fluctuations in the NE Iceland δ^{15}N$_{CBOM}$ chronology, which mirror such in the AMV index, can likely be explained by similar mechanisms described above. Different temperature regimes during positive and negative AMV phases were presumably also associated with a change in phytoplankton species composition which further affected the isotopic signals of diet and CBOM. As outlined further above, this is because each phytoplankton species carries a distinct δ^{15}N signature (Needoba et al., 2003) related to fractionation differences during nutrient uptake (Altabet and Francois, 1994).
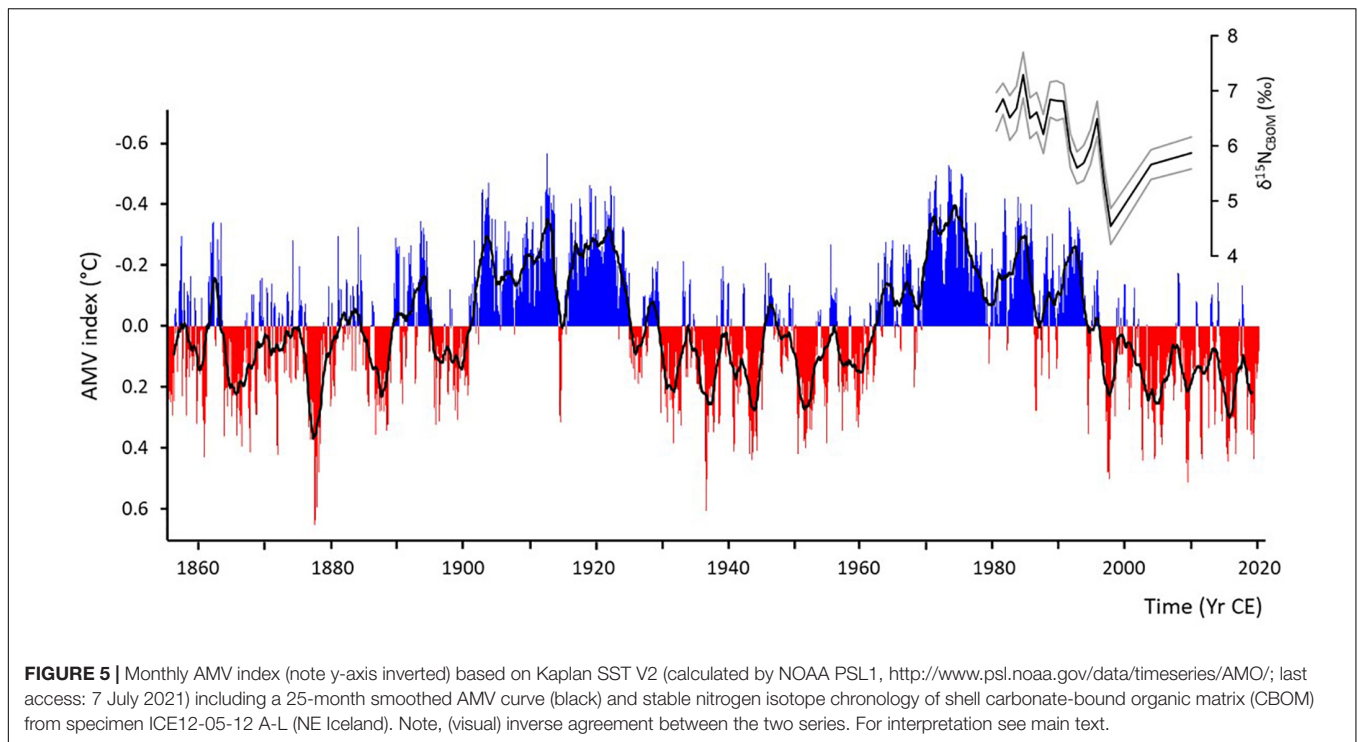
Variation of δ^{15}N$_{CBOM}$ in Modern Shells

In contrast to the studied subfossil specimens, ontogenetic δ^{15}N$_{CBOM}$ trends were more challenging to identify in the two live-collected modern specimens. Firstly, their lifespan barely exceeded 50 % of the period length of the multi-decadal variability. Existing trends may thus be masked or biased by the multidecadal fluctuations (viz. the strong δ^{15}N$_{CBOM}$ slope of the NE Iceland specimen; See section "Seasonal to Multidecadal Variability"). In addition, the two specimens lived at times during which anthropogenic environmental perturbations have already started to impact marine ecosystems and altered nitrogen dynamics in the ocean as evidenced by changes in δ^{15}N$_{TDN}$ (Häder et al., 2015). For instance, ocean acidification facilitated nitrogen fixation pathways (Hopkins et al., 2020) and resulted in ^{15}N-depleted ecosystems (Sigman and Casciotti, 2001; Gruber, 2008). It is therefore hard to tell if a negative δ^{15}N$_{CBOM}$ trend reflects a physiological or human-induced pH change or both. In addition, the influx of fertilizers to the coastal environments which the studied bivalves inhabited could have affected the δ^{15}N$_{TDN}$ signatures. The application of fertilizers which are typically ^{15}N-depleted in nitrate and/or ammonia could have had significant impacts on coastal δ^{15}N$_{TDN}$ and δ^{15}N$_{POM}$ (Heaton, 1986), and were consequently transferred through the food chains. Presumably, such an effect played a greater role in the Irish Sea than in more pristine waters of NE Iceland. The changes in δ^{15}N$_{CBOM}$ values from the anthropogenic impacts could have been compensated by the physiology-related δ^{15}N shift resulting in the nearly flat curve observed in the specimen from the Irish Sea. Hence, it is again stressed out that longer δ^{15}N$_{CBOM}$ chronologies, especially from the modern specimens, were needed to mathematically disentangle physiological and other factors.

Can δ^{15}N Values of Periostracum Serve as an Environmental Proxy?

In the great majority of hitherto studied bivalves, the δ^{15}N values of the soft tissues (specifically the muscle), periostracum and shell organic matrix were significantly correlated (O'Donnell et al., 2003; Carmichael et al., 2008; Delong and Thorp, 2009; Watanabe et al., 2009; Kovacs et al., 2010; Graniero et al., 2016, 2021; Darrow et al., 2017). This finding has opened new perspectives for studies evaluating the anthropogenic impact on ecosystems (Black et al., 2017; Fritts et al., 2017), hydrographical reconstructions (Whitney et al., 2019) and can be exploited in trophic (paleo)ecology, i.e., studies where soft tissues are not available or the agents used to preserve soft tissue altered the δ^{15}N signals (e.g., Versteegh et al., 2011).

Although the number of periostracum samples was limited in the present study, mostly due to preservation issues, data agreed at large with previous findings, specifically that by Whitney et al. (2019) on the same species: Time-series of δ^{15}N$_P$ and

FIGURE 5 | Monthly AMV index (note y-axis inverted) based on Kaplan SST V2 (calculated by NOAA PSL1, http://www.psl.noaa.gov/data/timeseries/AMO/; last access: 7 July 2021) including a 25-month smoothed AMV curve (black) and stable nitrogen isotope chronology of shell carbonate-bound organic matrix (CBOM) from specimen ICE12-05-12 A-L (NE Iceland). Note, (visual) inverse agreement between the two series. For interpretation see main text.

$\delta^{15}N_{CBOM}$ showed some agreement with each other, at least in the low-frequency domain, but with an offset (**Figure 4** and **Table 3**). CBOM was enriched in ^{15}N relative to periostracum, on average, by 0.86 (Irish Sea) to 2.07‰ (NE Iceland). We follow the interpretation by Whitney et al. (2019) and conclude that both materials, periostracum and shell organics capture similar signals, but are isotopically offset due to differing amino acid composition. However, what is difficult to understand is why the nitrogen isotopic offset between the periostracum and shell organics differed between the two specimens by 1.21‰ (**Figure 4** and **Table 3**). One possible explanation is that the historical shell was unknowingly treated with chemical agents or had been kept immersed in fluids that modified the isotope composition of the periostracum and/or the shell organics. As demonstrated in existing studies, storage in solutions can sometimes alter the amino acid composition and thus the isotope signatures (see reviews in Versteegh et al., 2011; Gillikin et al., 2017; Whiteman et al., 2019). For example, storage in formalin has been shown to increase $\delta^{15}N$ values of fish tissues by 0.5‰ irrespective of duration of immersion (Edwards et al., 2002. Two months of immersion in formalin, followed by 2 months in ethanol shifted the $\delta^{15}N$ values of fish muscle by 1.41‰ (Bosley and Wainright, 1999). In contrast, bivalve shell organic matrix became depleted in ^{15}N by up to 5.9‰ after storage in ethanol for 73 years (Versteegh et al., 2011). An alternative explanation would be the varying diets of *A. islandica* from the two different periods and locations. As Whitney et al. (2019) pointed out that the biomineral consisted of a higher proportion of trophic amino acids (e.g., Lys and Phe) compared with those in periostracum, it is possible to observe a higher $\delta^{15}N$ offset between shell and periostracum if the most recent NE Icelandic *A. islandica*

belonged to a higher trophic position, e.g., incorporating POM with a larger proportion of detritus deriving from animals of higher trophic levels.

Whereas it might be easier to measure a nearly pure organic material than a material which consists of approx. 95 to 99 wt% $CaCO_3$, we still feel that the shell organic matrix serves as the more useful and robust ecological archive. Firstly, sampling can be done more accurately in the shell carbonate, whereas dry periostracum is very brittle and flakes off from the shell in large pieces. It is therefore more difficult to sample periostracum without time-averaging. Secondly, periostracum is often not well preserved in old-grown specimens, even if live-collected, and missing in portions of the shell that formed during early ontogeny. In dry samples from museum collections, the periostracum is rarely well preserved on the entire shell surface, particularly if the samples have been touched frequently or were shuffled around. Thirdly, with increasing geological age, the likelihood to recover shells with intact periostracum decreases. The organic matrix of the shell is then the only remaining material that can be measured to reconstruct paleoecological conditions. Fourthly, contamination is a major concern. The periostracum protects the animal during lifetime against dissolution and microbial attack and as such is exposed to seawater. It is thus not surprising that epibionts and a rich microbiome settle on or even in the periostracum. Sometimes, sediment grains, diatoms, coccolithophorids etc. can be found trapped within the periostracum. It appears impossible to remove such contaminants effectively, and the use of oxidants and acids bears the danger to modify the nitrogen isotope signal of the periostracum unwittingly. In contrast, the shell carbonate, specifically the "inner core" of the shell, i.e., the iOSL is well

protected against contamination, and should, in our view, receive prioritized use.

SUMMARY AND CONCLUSION

The δ^{15}N values of the organic matrix in shells of the ocean quahog, *Arctica islandica* vary on seasonal to multidecadal time-scales and show a gradual decrease through lifetime by ca. 0.6‰ per century. The latter is most likely related to physiological changes of the bivalve. Should subsequent studied substantiate the findings herein and long δ^{15}N$_{CBOM}$ chronologies of *A. islandica* from other sites and time intervals also show the same decline through lifetime, these ontogenetic trends need to be mathematically removed before these data are used for ecological and environmental reconstructions. Presumably, the ontogenetic decline in δ^{15}N$_{CBOM}$ values results from a change in the type of proteins synthesized at different stages of life (Goodfriend and Weidman, 2001), i.e., a gradual shift from proteins rich in trophic (= strongly fractionating) amino acids (Glu, Asp, Ala) during youth toward proteins rich in source amino acids (Phe, Tyr, Lys) during adulthood. Alternative explanations include ontogenetic changes in food preferences and particle selection capabilities (i.e., a larger proportion of phytoplankton than organic detritus containing remains of organisms from higher trophic positions) or changes in the allocation of energy (to somatic growth during youth, and to reproduction and maintenance later during life) and associated changes in turnover rate. Aside from this ontogenetic trend, distinct multidecadal δ^{15}N$_{CBOM}$ variations (ca. 50 to 60 years) exist, modulated by quasi-decadal variability. These low-frequency fluctuations were likely governed by variations in nutrient supply mediated by the AMV/AMOC combined with changes in nitrate utilization by photoautotrophs and associated Rayleigh fractionation processes. To reliably identify and distinguish multidecadal variability and ontogenetic shifts, δ^{15}N$_{CBOM}$ time-series need to be sufficiently long. Furthermore, the presence or absence of ontogenetic trends requires specimens from different time intervals of the past and ideally also different localities and water depths. Otherwise, there is a danger to misinterpret directed environmental trends as ontogenetic shifts, or vice versa.

The stable nitrogen isotope composition of periostracum can offer an alternative means to assess ecological changes in the more recent past as long as chemical and biological contamination can be precluded. However, sampling of dry, brittle periostracum is challenging and prone to produce time-averaged chronologies. In the current study, the nitrogen isotope offset between contemporaneously formed shell organics and periostracum differed considerably (1.51‰) between two live-collected specimens, of which one lived in the mid-19th century and was obtained from a museum collection and the other lived

between the 1980s and 2012 CE. The difference may be explained by an unreported treatment of the historical shell with agents that modified the isotope signals of the periostracum or alternatively, be explained by the varying trophic levels of the two bivalves from different times and locality.

To address open questions raised herein and test hypotheses offered to explain the reasons for ontogenetic and multidecadal δ^{15}N$_{CBOM}$ variations, subsequent studies should: (1) employ compound-specific isotope techniques, and (2) compare high-resolution nitrogen isotope data from several old-grown, live-collected specimens with a plethora of environmental, ecological and biological data sets.

DATA AVAILABILITY STATEMENT

The original contributions presented in the study are included in the article/**Supplementary Material**, further inquiries can be directed to the corresponding author/s.

AUTHOR CONTRIBUTIONS

BS: conceptualization, funding acquisition, resources, sampling, data analysis, interpretation, visualization, and writing. QH: data analysis, interpretation, visualization, and writing. Both authors contributed to the article and approved the submitted version.

FUNDING

ACKNOWLEDGMENTS

SUPPLEMENTARY MATERIAL

The Supplementary Material for this article can be found online at: https://www.frontiersin.org/articles/10.3389/fmars.2021.748593/full#supplementary-material

REFERENCES

Abele, D., Strahl, J., Brey, T., and Philipp, E. E. R. (2008). Imperceptible senescence: ageing in the ocean quahog *Arctica islandica*. *Free Radic. Res.* 42, 474–480. doi: 10.1080/10715760802108849

Altabet, M. A., and Francois, R. (1994). Sedimentary nitrogen isotopic ratio as a recorder for surface ocean nitrate utilization. *Glob. Biogeochem. Cycles* 8, 103–116. doi: 10.1029/93GB03396

Altabet, M. A., Francois, R., Murray, D. W., and Prell, W. L. (1995). Climate-related variations in denitrification in the Arabian Sea from

sediment ^{15}N/^{14}N ratios. *Nature* 373, 506–509. doi: 10.1038/3735 06a0

Baptista, M., Repolho, T., Maulvault, A. L., Lopes, V. M., Narciso, L., Marques, A., et al. (2014). Temporal dynamics of amino and fatty acid composition in the razor clam *Ensis siliqua* (Mollusca: Bivalvia). *Helgol. Mar. Res.* 68, 465–482. doi: 10.1007/s10152-014-0402-7

Barton, A. D., Greene, C. H., Monger, B. C., and Pershing, A. J. (2003). The Continuous Plankton Recorder survey and the North Atlantic Oscillation: interannual- to multidecadal-scale patterns of phytoplankton variability in the North Atlantic Ocean. *Prog. Oceanogr.* 58, 337–358. doi: 10.1016/j.pocean.2003.08.012

Barton, A. D., Lozier, M. S., and Williams, R. G. (2014). Physical controls of variability in North Atlantic phytoplankton communities. *Limnol. Oceanogr.* 60, 181–197. doi: 10.1002/lno.10011

Benedetti, F., Jalabert, L., Sourisseau, M., Becker, B., Cailliau, C., Desnos, C., et al. (2019). The seasonal and inter-annual fluctuations of plankton abundance and community structure in a North Atlantic marine protected area. *Front. Mar. Sci.* 6:214. doi: 10.3389/fmars.2019.00214

Birkel, S. D., Mayewski, P. A., Maasch, K. A., Auger, J., and Lyon, B. (2016). *A Volcanic Wind-Stress Origin of the Atlantic Multidecadal Oscillation. AGU Fall Meeting Abstracts, A21B-0030*. Washington, DC: American Geophysical Union.

Black, H. D., Andrus, C. F. T., Lambert, W. J., Rick, T. C., and Gillikin, D. P. (2017). δ15N values in *Crassostrea virginica* shells provides early direct evidence for nitrogen loading to Chesapeake Bay. *Sci. Rep.* 7:44241. doi: 10.1038/srep44241

Bosley, K. L., and Wainright, S. C. (1999). Effects of preservatives and acidification on the stable isotope ratios (^{15}N:^{14}N, ^{13}C:^{12}C) of two species of marine animals. *Can. J. Fish. Aquat. Sci.* 56, 2181–2185. doi: 10.1139/f99-153

Bronk, D. A., and Glibert, P. M. (1993). Application of a ^{15}N tracer method to the study of dissolved organic nitrogen uptake during spring and summer in Chesapeake Bay. *Mar. Biol.* 115, 501–508. doi: 10.1007/BF00349849

Butler, P. G., Wanamaker, A. D. Jr., Scourse, J. D., Richardson, C. A., and Reynolds, D. J. (2013). Variability of marine climate on the North Icelandic shelf in a 1357-year proxy archive based on growth increments in the bivalve *Arctica islandica*. *Palaeogeogr. Palaeoclimatol. Palaeoecol.* 373, 141–151. doi: 10.1016/j.palaeo.2012.01.016

Cabana, G., and Rasmussen, J. B. (1996). Comparison of aquatic food chains using nitrogen isotopes. *Proc. Natl. Acad. Sci. U.S.A.* 93, 10844–10847. doi: 10.1073/pnas.93.20.10844

Cargnelli, L. M., Griesbach, S. J., Packer, D. B., and Weissberger, E. (1999). *Ocean Quahog, Arctica islandica, Life History and Habitat Characteristics. NOAA Technical Memorandum NMFS-NE-148*. Woods Hole, MA: U.S. Dept. of Commerce, National Oceanic and Atmospheric Administration, National Marine Fisheries Service, 1–12.

Carmichael, R. H., Annett, B., and Valiela, I. (2004). Nitrogen loading to Pleasant Bay, Cape Cod: application of models and stable isotopes to detect incipient nutrient enrichment of estuaries. *Mar. Pollut. Bull.* 48, 137–143. doi: 10.1016/S0025-326X(03)00372-2

Carmichael, R. H., Hattenrath, T., Valiela, I., and Michener, R. H. (2008). Nitrogen stable isotopes in the shell of *Mercenaria mercenaria* trace wastewater inputs from watersheds to estuarine ecosystems. *Aquat. Biol.* 4, 99–111. doi: 10.3354/ab00106

Chikaraishi, Y., Kashiyama, Y., Ogawa, N. O., Kitazato, H., and Ohkouchi, N. (2007). Metabolic control of nitrogen isotope composition of amino acids in macroalgae and gastropods: implications for aquatic food web studies. *Mar. Ecol. Prog. Ser.* 342, 85–90. doi: 10.3354/meps342085

Chikaraishi, Y., Ogawa, N. O., Kashiyama, Y., Takano, Y., Suga, H., Tomitani, A., et al. (2009). Determination of aquatic food-web structure based on compound-specific nitrogen isotopic composition of amino acids. *Limnol. Oceanogr. Methods* 7, 740–750. doi: 10.4319/lom.2009.7.740

Darrow, E. S., Carmichael, R. H., Andrus, C. F. T., and Jackson, H. E. (2017). From middens to modern estuaries, oyster shells sequester source-specific nitrogen. *Geochim. Cosmochim. Acta* 202, 39–56. doi: 10.1016/j.gca.2016.12.023

Das, S., Judd, E. J., Uveges, B. T., Ivany, L. C., and Junium, C. K. (2021). Variation in δ^{15}N from shell-associated organic matter in bivalves: implications for studies of modern and fossil ecosystems. *Palaeogeogr. Palaeoclimatol. Palaeoecol.* 562:110076. doi: 10.1016/j.palaeo.2020.110076

Delong, M. D., and Thorp, J. H. (2009). Mollusc shell periostracum as an alternative to tissue in isotopic studies. *Limnol. Oceanogr. Methods* 7, 436–441. doi: 10.4319/lom.2009.7.436

Delworth, T. L., and Mann, M. E. (2000). Observed and simulated multidecadal variability in the Northern Hemisphere. *Clim. Dyn.* 16, 661–676. doi: 10.1007/s003820000075

DeNiro, M. J., and Epstein, S. (1981). Influence of diet on the distribution of nitrogen isotopes in animals. *Geochim. Cosmochim. Acta* 45, 341–351. doi: 10.1016/0016-7037(81)90244-1

Doherty, J. M., Williams, B., Kline, E., Adey, W., and Thibodeau, B. (2021). Climate-modulated nutrient conditions along the Labrador Shelf: evidence from nitrogen isotopes in a six-hundred-year-old crustose coralline alga. *Paleoceanogr. Paleoclimatol.* 36:e2020A004149. doi: 10.1029/2020PA004149

Duce, R. A., LaRoche, J., Altieri, K., Arrigo, K. R., Baker, A. R., Capone, D. G., et al. (2008). Impacts of atmospheric anthropogenic nitrogen on the open ocean. *Science* 320, 893–897. doi: 10.1126/science.1150369

Duprey, N. N., Wang, T. X., Kim, T., Cybulski, J. D., Vonhof, H. B., Crutzen, P. J., et al. (2020). Megacity development and the demise of coastal coral communities: evidence from coral skeleton δ^{15}N records in the Pearl river estuary. *Glob. Change Biol.* 26, 1338–1353. doi: 10.1111/gcb.14923

Edwards, M. S., Turner, T. F., and Sharp, Z. D. (2002). Short- and long-term effects of fixation and preservation on stable isotope values (δ^{13}C, δ^{15}N, δ^{34}S) of fluid-preserved museum specimens. *Copeia* 2002, 1106–1112. doi: 10.2307/1448532

Edwards, M., Reid, P. C., and Planque, B. (2001). Long-term and regional variability of phytoplankton biomass in the Northeast Atlantic (1960–1995). *ICES J. Mar. Sci.* 58, 39–49. doi: 10.1006/jmsc.2000.0987

Ellis, G. (2012). *Compound-Specific Stable Isotopic Analysis of Protein Amino Acids: Ecological Applications in Modern and Ancient Systems*. Ph.D. thesis. Gainesville, FL: University of Florida.

Emmery, A., Lefebvre, S., Alunno-Bruscia, M., and Kooijman, S. A. L. M. (2011). Understanding the dynamics of δ^{13}C and δ^{15}N in soft tissues of the bivalve *Crassostrea gigas* facing environmental fluctuations in the context of Dynamic Energy Budgets (DEB). *J. Sea Res.* 66, 361–371. doi: 10.1016/j.seares.2011.08.002

Erlenkeuser, H. (1976). ^{14}C and ^{13}C isotope concentration in modern marine mussels from sedimentary habitats. *Sci. Nat.* 63:338. doi: 10.1007/bf00597312

Fox, J., and Weisberg, S. (2019). *An R Companion to Applied Regression*, 3rd Edn. Thousand Oaks CA: Sage.

Fritts, A. K., Fritts, M. W., Haag, W. R., DeBoer, J. A., and Casper, A. F. (2017). Freshwater mussel shells (Unionidae) chronicle changes in a North American river over the past 1000 years. *Sci. Total Environ.* 575, 199–206. doi: 10.1016/j.scitotenv.2016.09.225

Fry, B. (1988). Food web structure on Georges Bank from stable C, N, and S isotopic compositions. *Limnol. Oceanogr.* 33, 1182–1190. doi: 10.4319/lo.1988.33.5.1182

Geeraert, N., Duprey, N. N., McIlroy, S. E., Thompson, P. D., Goldstein, B. R., LaRoche, C., et al. (2020). The anthropogenic nitrogen footprint of a tropical lagoon: spatial variability in *Padina* sp. δ^{15}N values. *Pac. Sci.* 74, 19–29. doi: 10.2984/74.1.2

Gillikin, D. P., Lorrain, A., Jolivet, A., Kelemen, Z., Chauvaud, L., and Bouillon, S. (2017). High-resolution nitrogen stable isotope sclerochronology of bivalve shell carbonate-bound organics. *Geochim. Cosmochim. Acta* 200, 55–66. doi: 10.1016/j.gca.2016.12.008

Goodfriend, G. A., and Weidman, C. R. (2001). Ontogenetic trends in aspartic acid racemization and amino acid composition within modern and fossil shells of the bivalve *Arctica*. *Geochim. Cosmochim. Acta* 65, 1921–1932. doi: 10.1016/S0016-7037(01)00564-6

Goulletquer, P., and Wolowicz, M. (1989). The shell of *Cardium edule, Cardium glaucum* and *Ruditapes philippinarum*: organic content, composition and energy value, as determined by different methods. *J. Mar. Biol. Assoc. U. K.* 69, 563–572. doi: 10.1017/S0025315400030976

Graniero, L. E., Gillikin, D. P., Surge, D., Kelemen, Z., and Bouillon, S. (2021). Assessing δ^{15}N values in the carbonate-bound organic matrix and periostracum of bivalve shells as environmental archives. *Palaeogeogr. Palaeoclimatol. Palaeoecol.* 564:110108. doi: 10.1016/j.palaeo.2020.110108

Graniero, L. E., Grossman, E. L., and O'Dea, A. (2016). Stable isotopes in bivalves as indicators of nutrient source in coastal waters in the Bocas del Toro Archipelago, Panama. *PeerJ* 4:e2278. doi: 10.7717/peerj.2278

Gruber, N. (2008). "The marine nitrogen cycle: overview and challenges," in *Nitrogen in the Marine Environment*, eds D. G. Capone, D. A. Bronk, M. R.

Mulholland, and E. J. Carpenter (Cambridge, MA: Academic Press), doi: 10.1016/B978-0-12-372522-6.00001-3

Häder, D. P., Gao, K., and Tyagi, M. B. (2015). Interactions of anthropogenic stress factors on marine phytoplankton. *Front. Environ. Sci.* 3:14. doi: 10.3389/fenvs.2015.00014

Hansen, J. H., Hedeholm, R. B., Sünksen, K., Christensen, J. T., and Grønkjær, P. (2012). Spatial variability of carbon (δ^{13}C) and nitrogen (δ^{15}N) stable isotope ratios in an Arctic marine food web. *Mar. Ecol. Prog. Ser.* 467, 47–59. doi: 10.3354/meps09945

Heaton, T. H. E. (1986). Isotopic studies of nitrogen pollution in the hydrosphere and atmosphere: a review. *Chem. Geol. Isot. Geosci. Sect.* 59, 87–102. doi: 10.1016/0168-9622(86)90059-x

Heaton, T. J., Köhler, P., Butzin, M., Bard, E., Reimer, R. W., Austin, W. E. N., et al. (2020). Marine20—the marine radiocarbon age calibration curve (0–55,000 cal BP). *Radiocarbon* 62, 779–820. doi: 10.1017/RDC.2020.68

Henson, S. A., Dunne, J. P., and Sarmiento, J. (2009). Decadal variability in North Atlantic phytoplankton blooms. *J. Geophys. Res.* 114:C04013. doi: 10.1029/2008JC005139

Hobson, K. A., and Welch, H. E. (1992). Determination of trophic relationships within a high Arctic marine food web using δ^{13}C and δ^{15}N analysis. *Mar. Ecol. Prog. Ser.* 84, 9–18. doi: 10.3354/meps084009

Hopkins, F. E., Suntharalingam, P., Gehlen, M., Andrews, O., Archer, S. D., Bopp, L., et al. (2020). The impacts of ocean acidification on marine trace gases and the implications for atmospheric chemistry and climate. *Proc. Math. Phys. Eng. Sci.* 476:20190769. doi: 10.1098/rspa.2019.0769

Ishikawa, N. F. (2018). Use of compound-specific nitrogen isotope analysis of amino acids in trophic ecology: assumptions, applications, and implications. *Ecol. Res.* 33, 825–837. doi: 10.1007/s11284-018-1616-y

Jones, D. S. (1980). Annual cycle of shell growth increment formation in two continental shelf bivalves and its paleoecologic significance. *Paleobiology* 6, 331–340. doi: 10.1017/S0094837300006837

Josefson, A. B., Jensen, J. N., Nielsen, T. G., and Rasmussen, B. (1995). Growth parameters of a benthic suspension feeder along a depth gradient across the pycnocline in the southern Kattegat, Denmark. *Mar. Ecol. Prog. Ser.* 125, 107–115. doi: 10.3354/meps125107

Kang, C. K., Sauriau, P. G., Richard, P., and Blanchard, G. F. (1999). Food sources of the infaunal suspension-feeding bivalve *Cerastoderma edule* in a muddy sandflat of Marennes-Oléron Bay, as determined by analyses of carbon and nitrogen stable isotopes. *Mar. Ecol. Prog. Ser.* 187, 147–158. doi: 10.3354/meps187147

Keenlyside, N. S., Latif, M., Jungclaus, J., Kornblueh, L., and Roeckner, E. (2008). Advancing decadal-scale climate prediction in the North Atlantic sector. *Nature* 453, 84–88. doi: 10.1038/nature06921

Kiørboe, T., and Møhlenberg, F. (1981). Particle selection in suspension-feeding bivalves. *Mar. Ecol. Prog. Ser.* 5, 291–296. doi: 10.3354/meps005291

Kovacs, C. J., Daskin, J. H., Patterson, H., and Carmichael, R. H. (2010). *Crassostrea virginica* shells record local variation in wastewater inputs to a coastal estuary. *Aquat. Biol.* 9, 77–84. doi: 10.3354/ab00228

LeBlanc, C. (1989). *Terrestrial Input to Estuarine Bivalves as Measured by Multiple Stable Isotopes Tracers.* Ph.D. thesis. Montreal, QC: McMaster University.

Lehmann, N., Kienast, M., Granger, J., Bourbonnais, A., Altabet, M. A., and Tremblay, J. (2019). Remote western Arctic nutrients fuel remineralization in deep Baffin Bay. *Glob. Biogeochem. Cycles* 33, 649–667. doi: 10.1029/2018GB006134

Lueders-Dumont, J. A., Wang, X. T., Jensen, O. P., Sigman, D. M., and Ward, B. B. (2018). Nitrogen isotopic analysis of carbonate-bound organic matter in modern and fossil fish otoliths. *Geochim. Cosmochim. Acta* 224, 200–222. doi: 10.1016/j.gca.2018.01.001

Mann, M. E., Steinmann, B. A., Brouillette, D. J., and Miller, S. K. (2021). Multidecadal climate oscillations during the past millennium driven by volcanic forcing. *Science* 371, 1014–1019. doi: 10.1126/science.abc5810

Marali, S., and Schöne, B. R. (2015). Oceanographic control on shell growth of *Arctica islandica* (Bivalvia) in surface waters of Northeast Iceland – implications for paleoclimate reconstructions. *Palaeogeogr. Palaeoclimatol. Palaeoecol.* 420, 138–149. doi: 10.1016/j.palaeo.2014.12.016

Marconi, D., Weigand, M. A., and Sigman, D. M. (2019). Nitrate isotopic gradients in the north Atlantic Ocean and the nitrogen isotopic composition of sinking organic matter. *Deep Sea Res. I Oceanogr. Res. Pap.* 145, 109–124. doi: 10.1016/j.dsr.2019.01.010

McClelland, J. W., and Montoya, J. P. (2002). Trophic relationships and the nitrogen isotopic composition of amino acids in plankton. *Ecology* 83, 2173–2180.

Minagawa, M., and Wada, E. (1984). Stepwise enrichment of ^{15}N along food chains: further evidence and the relation between δ^{15}N and animal age. *Geochim. Cosmochim. Acta* 48, 1135–1140. doi: 10.1016/0016-7037(84)90204-7

Misarti, N., Gier, E., Finney, B., Barnes, K., and McCarthy, M. (2017). Compound-specific amino acid δ^{15}N values in archaeological shell: assessing diagenetic integrity and potential for isotopic baseline reconstruction. *Rapid Commun. Mass Spectrom.* 31, 1881–1891. doi: 10.1002/rcm.7963

Miyake, Y., and Wada, E. (1967). The abundance ratio of ^{15}N/^{14}N in marine environments. *Rec. Oceanogr. Works Jpn. New Ser.* 9, 37–53.

Montoya, J. P., and McCarthy, J. J. (1995). Isotopic fractionation during nitrate uptake by phytoplankton grown in continuous culture. *J. Plankton Res.* 17, 439–464. doi: 10.1093/plankt/17.3.439

Needoba, J. A., Waser, N. A., Harrison, P. J., and Calvert, S. E. (2003). Nitrogen isotope fractionation in 12 species of marine phytoplankton during growth on nitrate. *Mar. Ecol. Prog. Ser.* 255, 81–91. doi: 10.3354/meps255081

O'Donnell, T. H., Macko, S. A., Chou, J., Davis-Hartten, K. L., and Wehmiller, J. F. (2003). Analysis of δ^{13}C, δ^{15}N, and δ^{34}S in organic matter from the biominerals of modern and fossil *Mercenaria* spp. *Org. Geochem.* 34, 165–183. doi: 10.1016/S0146-6380(02)00160-2

Ohkouchi, N., Ogawa, N. O., Chikaraishi, Y., Tanaka, H., and Wada, E. (2015). Biochemical and physiological bases for the use of carbon and nitrogen isotopes in environmental and ecological studies. *Prog. Earth Planet. Sci.* 2, 1–17. doi: 10.1186/s40645-015-0032-y

Perkins, M. J., McDonald, R. A., van Veen, F. J. F., Kelly, S. D., Rees, G., and Bearhop, S. (2014). Application of nitrogen and carbon stable isotopes (δ^{15}N and δ^{13}C) to quantify food chain length and trophic structure. *PLoS One* 9:e93281. doi: 10.1371/journal.pone.0093281

Phillips, D. L., and Koch, P. L. (2002). Incorporating concentration dependence in stable isotope mixing models. *Oecologia* 130, 114–125. doi: 10.1007/s004420100786

Polissar, P. J., Fulton, J. M., Junium, C. K., Turich, C. C., and Freeman, K. H. (2009). Measurement of ^{13}C and ^{15}N isotopic composition on nanomolar quantities of C and N. *Anal. Chem.* 81, 755–763. doi: 10.1021/ac801370c

Popp, B. N., Graham, B. S., Olson, R. J., Hannides, C. C. S., Lott, M. J., López-Ibarra, G. A., et al. (2007). Insight into the trophic ecology of yellowfin tuna, *Thunnus albacares*, from compound-specific nitrogen isotope analysis of proteinaceous amino acids. *Terr. Ecol.* 1, 173–190. doi: 10.1016/s1936-7961(07)01012-3

Post, D. M. (2002). Using stable isotopes to estimate trophic position: models, methods, and assumptions. *Ecology* 83, 703–718.

R Core Team (2021). *R: A Language and Environment for Statistical Computing.* Vienna: R Foundation for Statistical Computing.

Rossi, F., Herman, P. M. J., and Middelburg, J. J. (2004). Interspecific and intraspecific variation of δ^{13}C and δ^{15}N in deposit- and suspension-feeding bivalves (*Macoma balthica* and *Cerastoderma edule*): evidence of ontogenetic changes in feeding mode of *Macoma balthica*. *Limnol. Oceanogr.* 49, 408–414. doi: 10.4319/lo.2004.49.2.0408

Schlacher, T. A., and Connolly, R. M. (2014). Effects of acid treatment on carbon and nitrogen stable isotope ratios in ecological samples: a review and synthesis. *Methods Ecol. Evol.* 5, 541–550. doi: 10.1111/2041-210X.12183

Schlesinger, M. E., and Ramankutty, N. (1994). An oscillation in the global climate system of period 65-70 years. *Nature* 367, 723–726. doi: 10.1038/367723a0

Schöne, B. R. (2013). *Arctica islandica* (Bivalvia): a unique paleoenvironmental archive of the northern North Atlantic Ocean. *Glob. Planet. Change* 111, 199–225. doi: 10.1016/j.gloplacha.2013.09.013

Schöne, B. R., Fiebig, J., Pfeiffer, M., Gleβ, R., Hickson, J., Johnson, A. L. A., et al. (2005a). Climate records from a bivalved Methuselah (*Arctica islandica*, Mollusca; Iceland). *Palaeogeogr. Palaeoclimatol. Palaeoecol.* 228, 130–148. doi: 10.1016/j.palaeo.2005.03.049

Schöne, B. R., Pfeiffer, M., Pohlmann, T., and Siegismund, F. (2005b). A seasonally resolved bottom water temperature record for the period of AD 1866–2002 based on shells of *Arctica islandica* (Mollusca, North Sea). *Int. J. Climatol.* 25, 947–962. doi: 10.1002/joc.1174

Schöne, B. R., Schmitt, K., and Maus, M. (2017). Effects of sample pretreatment and external contamination on bivalve shell and Carrara marble δ^{18}O and δ^{13}C signatures. *Palaeogeogr. Palaeoclimatol. Palaeoecol.* 484, 22–32. doi: 10.1016/j.palaeo.2016.10.026

Serna, A., Pätsch, J., Dähnke, K., Wiesner, M. G., Hass, H. C., Zeiler, M., et al. (2010). History of anthropogenic nitrogen input to the German Bight/SE North Sea as reflected by nitrogen isotopes in surface sediments, sediment cores and hindcast models. *Cont. Shelf Res.* 30, 1626–1638. doi: 10.1016/j.csr.2010.06.010

Sherwood, O. A., Lehmann, M. F., Schubert, C. J., Scott, D. B., and McCarthy, M. D. (2011). Nutrient regime shift in the western North Atlantic indicated by compound-specific δ^{15}N of deep-sea gorgonian corals. *Proc. Natl. Acad. Sci. U.S.A.* 108, 1011–1015. doi: 10.1073/pnas.1004904108

Shumway, S. E., Cucci, T. L., Newell, R. C., and Yentsch, C. M. (1985). Particle selection, ingestion, and absorption in filter-feeding bivalves. *J. Exp. Mar. Biol. Ecol.* 91, 77–92. doi: 10.1016/0022-0981(85)90222-9

Sigman, D. M., and Casciotti, K. L. (2001). "Nitrogen isotopes in the ocean," in *Encyclopedia of Ocean Sciences*, ed. J. H. Steele (London: Academic Press), 1884–1894. doi: 10.1006/rwos.2001.0172

Simon, M., Grossart, H.-P., Schweitzer, B., and Ploug, H. (2002). Microbial ecology of organic aggregates in aquatic ecosystems. *Aquat. Microb. Ecol.* 28, 175–211. doi: 10.3354/ame028175

Sverdrup, H. U. (1953). On conditions for the vernal blooming of phytoplankton. *J. Cons. Int. Explor. Mer.* 18, 287–295. doi: 10.1093/icesjms/18.3.287

Thompson, D. R., Furness, R. W., and Lewis, S. A. (1995). Diets and long-term changes in δ^{15}N and δ^{13}C values in northern fulmars *Fulmarus glacialis* from two northeast Atlantic colonies. *Mar. Ecol. Prog. Ser.* 125, 3–11. doi: 10.3354/meps125003

Thompson, I., Jones, D. S., and Dreibelbis, D. (1980). Annual internal growth banding and life history of the ocean quahog *Arctica islandica* (Mollusca: Bivalvia). *Mar. Biol.* 57, 24–34. doi: 10.1007/bf00420964

Thorarinsdóttir, G. G., and Steingrímsson, S. A. (2000). Size and age at sexual maturity and sex ratio in ocean quahog, *Arctica islandica* (Linnaeus, 1767), off northwest Iceland. *J. Shellfish Res.* 19, 943–947.

Tue, N. T., Hamaoka, H., Sogabe, A., Quy, T. D., Nhuan, M. T., and Omori, K. (2012). Food sources of macro-invertebrates in an important mangrove ecosystem of Vietnam determined by dual stable isotope signatures. *J. Sea Res.* 72, 14–21. doi: 10.1016/j.seares.2012.05.006

Verdugo, P., Alldredge, A. L., Azam, F., Kirchman, D. L., Passow, U., and Santschi, P. H. (2004). The oceanic gel phase: a bridge in the DOM–POM continuum. *Mar. Chem.* 92, 67–85. doi: 10.1016/j.marchem.2004.06.017

Versteegh, E. A., Gillikin, D. P., and Dehairs, F. (2011). Analysis of δ^{15}N values in mollusk shell organic matrix by elemental analysis/isotope ratio mass spectrometry without acidification: an evaluation and effects of long-term

preservation. *Rapid Commun. Mass Spectrom.* 25, 675–680. doi: 10.1002/rcm.4905

Voss, M., Emeis, K.-C., Hille, S., Neumann, T., and Dippner, J. W. (2005). Nitrogen cycle of the Baltic Sea from an isotopic perspective. *Glob. Biogeochem. Cycles* 19:GB3001. doi: 10.1029/2004GB00233

Wanamaker, A. D. Jr., Heinemeier, J., Scourse, J. D., Richardson, C. A., Butler, P. G., Eiríksson, J., et al. (2008). Very long-lived mollusks confirm 17*th* century AD tephra-based radiocarbon reservoir ages for North Icelandic shelf waters. *Radiocarbon* 50, 399–412. doi: 10.1017/s0033822200053510

Wang, X. T., Cohen, A. L., Luu, V., Ren, H., Su, Z., Haug, G. H., et al. (2018). Natural forcing of the North Atlantic nitrogen cycle in the Anthropocene. *Proc. Natl. Acad. Sci. U.S.A.* 115, 10606–10611. doi: 10.1073/pnas.1801049115

Watanabe, S., Kodama, M., and Fukudam, M. (2009). Nitrogen stable isotope ratio in the manila clam, *Ruditapes philippinarum*, reflects eutrophication levels in tidal flats. *Mar. Pollut. Bull.* 58, 1447–1453. doi: 10.1016/j.marpolbul.2009.06.018

Whiteman, J. P., Elliot Smith, E. A., Besser, A. C., and Newsome, S. D. (2019). A guide to using compound-specific stable isotope analysis to study the fates of molecules in organisms and ecosystems. *Diversity* 11:8. doi: 10.3390/d11010008

Whitney, N. M., Johnson, B. J., Dostie, P. T., Luzier, K., and Wanamaker, A. D. Jr. (2019). Paired bulk organic and individual amino acid δ^{15}N analyses of bivalve shell periostracum: a paleoceanographic proxy for water source variability and nitrogen cycling processes. *Geochim. Cosmochim. Acta* 254, 67–85. doi: 10.1016/j.gca.2019.03.019

Zhang, R., Sutton, R., Danabasoglu, G., Kwon, Y. O., Marsh, R., Yeager, S. G., et al. (2019). A review of the role of the Atlantic meridional overturning circulation in Atlantic multidecadal variability and associated climate impacts. *Rev. Geophys.* 57, 316–375. doi: 10.1029/